Overdamped phase diffusion in hBN encapsulated graphene Josephson junctions

J. Tang,[1] M. T. Wei,[2] A. Sharma,[1,3] E. G. Arnault,[4] A. Seredinski,[5] Y. Mehta,[6] K. Watanabe,[7] T. Taniguchi,[7] F. Amet,[6] and I. Borzenets[1,3,*]

[1]*Department of Physics, City University of Hong Kong, Kowloon, Hong Kong SAR*
[2]*Joint Quantum Institute, University of Maryland, Maryland 20742, USA*
[3]*Department of Physics and Astronomy, Texas A&M University, Texas 77843, USA*
[4]*Department of Physics, Duke University, Durham, North Carolina 27708, USA*
[5]*Department of Sciences, Wentworth Institute of Technology, Boston, Massachusetts 02115, USA*
[6]*Department of Physics and Astronomy, Appalachian State University, Boone, North Carolina 28607, USA*
[7]*Advanced Materials Laboratory, National Institute for Materials Science, Tsukuba 305-0044, Japan*

(Received 29 December 2020; revised 3 May 2022; accepted 13 May 2022; published 10 June 2022)

We investigate the zero-bias behavior of Josephson junctions made of encapsulated graphene boron nitride heterostructures in the long ballistic junction regime. For temperatures down to 2.7 K, the junctions appear non-hysteretic with respect to the switching and retrapping currents I_C and I_R. A small nonzero resistance is observed even around zero-bias current and scales with temperature as dictated by the phase diffusion mechanism. By varying the graphene carrier concentration we are able to confirm that the observed phase diffusion mechanism follows the trend for an overdamped Josephson junction. This is in contrast with the majority of graphene-based junctions which are underdamped and shorted by the environment at high frequencies.

DOI: 10.1103/PhysRevResearch.4.023203

Graphene-based superconductor-normal metal-superconductor Josephson junctions (JJs) have been a popular medium of choice for studying the fundamentals [1–11] as well as applications [12–17] of superconducting devices for more than a decade. However, the full spectrum and consequences of the interactions between the graphene Josephson junction and the environment have not been fully mapped. For example, the observed critical current I_C of graphene Josephson junctions is consistently suppressed compared to theoretical predictions; leading to postulations that the junctions are severely underdamped [5,6,9,10,18], despite the relatively low hysteresis between the switching I_S and the retrapping I_R currents. The effect of a junction's environment on its dynamics can be directly investigated by looking at the statistical distribution of the switching current I_S [7–9,19,20], however, such measurements add significant complexity and are not typically practical for device characterization. Alternatively, the damping regime of the junction can be assessed via the measurement of zero-bias resistance arising from the phase diffusion mechanism [5,18,21–25]. Analysis of the phase diffusion mechanism can be performed via the common I–V bias measurements, and among other things, allows one to extract the Josephson energy without measuring the critical current. Previous works have shown that the vast majority of graphene-based JJs are underdamped [5,6,9,10]; this is often attributed to the large capacitance generated by the bonding pads and leads. Therefore, a scheme for designing and characterizing overdamped graphene Josephson junctions is worthwhile.

In this paper we report on Josephson junctions made from hexagonal boron nitride (hBN) encapsulated graphene with molybdenum rhenium (MoRe) alloy superconducting contacts [14,15,26]. These devices are governed by ballistic electron transport and have been found to be in the intermediate to long-junction regime [9] (see Appendices A and C). Here, the MoRe contacts terminate shortly after the active region and are connected to the bonding pads via thin gold leads. Moreover, the MoRe contacts exhibit a high level of oxidation, introducing disorder, decreasing the Cooper pair density and, in turn, increasing the kinetic inductance. This kinetic inductance acts to insulate the Josephson junction from the effect of the large bonding pad capacitance (see Appendix B). The junctions were measured at temperatures between 2.7 and 7 K where a clear phase diffusion governed zero-bias resistance can be observed [5,18,21–25]. However, for these devices, when changing the carrier concentration via the backgate, the zero-bias resistance follows the trend expected for overdamped junctions [5,25,27]. Thus, we conclude that we have demonstrated ballistic graphene Josephson junction in the overdamped regime.

Graphene is made using the exfoliation method [28] and is encapsulated in hBN using the pickup method [26]. Using CHF_3/O_2 plasma, the hBN-graphene-hBN stack is etched thorough in order to make quasi-one-dimensional electrical contacts with superconducting electrodes [14]. MoRe alloy electrodes are deposited onto the device using DC sputtering

*Corresponding author: borzenets@tamu.edu

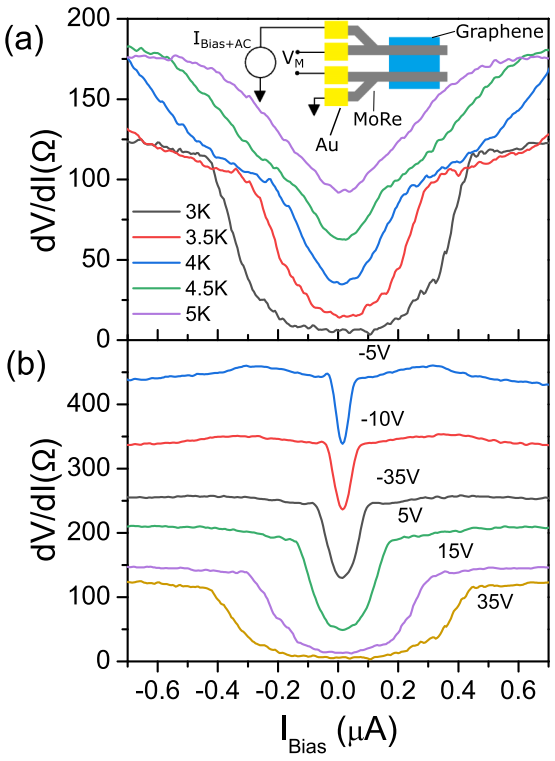

FIG. 1. The inset: The measurement schematic of the device. Differential resistance dV/dI as a function of DC bias current I_{Bias}. The current is swept from negative to positive. Panel (a) shows dV/dI curves for different temperatures. The gate voltage here is set to 35 V. Panel (b) shows dV/dI curves for different applied gate voltages. The temperature here is 3 K. Note that there is no observable hysteresis between the switching and the retrapping current. (The curves appear symmetrical about zero bias). Moreover, all curves feature a measurable zero-bias resistance R_0 arising from the phase diffusion mechanism.

with the approximate thickness of 100–120 nm. (Previous work has demonstrated that MoRe alloy electrodes in a quasi-one-dimensional contact configuration result in electrical contact transparencies of up to 90% [9,14].) The bonding pads and thin metal leads making contact to MoRe are made of Cr/Au (5/110 nm). Here, we present data on the device of length $L = 500$ nm (the distance between MoRe contacts) and the width $W = 3$ μm (see Appendix A).

The device is measured in a home-made cryocooler with a base temperature of 2.5 K, which is isolated via both a heat shield and RC filters placed at the low-temperature stage. Josephson junction resistance is measured using the lock-in method with a four-probe geometry [Fig. 1(a) inset]. The junction is biased by a variable DC current with a small AC excitation of 5 nA. The voltage across the junction is amplified using a custom differential preamp prior to being fed into the lock in. The gate voltage applied to the back of the 300-nm SiO_2 oxide layer is used to control the carrier density of graphene. Figure 1 presents the differential resistance dV/dI as a function of applied DC bias current I_{Bias}. All the curves show two transition points as the bias current is swept from a large negative value to a large positive value. The absolute value of the current on the negative side below which the junction becomes superconducting is the retrapping current I_R, i.e., $|I_{Bias}| = I_R$. On the positive side, the junction transitions from the superconducting to the normal state at the switching current I_S [18]. Figure 1(a) shows resistance versus I_{Bias} for different temperatures with the backgate voltage set to 35 V. Figure 1(b) shows the resistance versus bias current for different gate voltages taken at 3 K. In both cases, the switching and retrapping currents I_S and I_R follow the expected trends: falling exponentially with increasing temperature and increasing with gate voltage away from the Dirac point with the hole conduction regime exhibiting a suppressed critical current due to the effects of contact doping [5,6,9]. Moreover, the trend of I_S with respect to temperature T follows that expected for ballistic Josephson junctions in the long junction regime (see Appendix C) [9].

For all tested gates and temperatures we do not observe a difference between I_S and I_R, i.e., there is no observable hysteresis. The vast majority of previously reported graphene Josephson junctions exhibit hysteresis between the switching and retrapping currents (with $I_S > I_R$) even for temperatures above 3 K. Whereas certain works attribute the existence of hysteresis to self-heating of the junction [13,29], it has also been shown that most of the graphene Josephson junctions exhibit underdamped behavior [5,6,9,10]. However, it is still possible that hysteresis has been smeared out due to temperature [18] as opposed to overdamped junction behavior.

Therefore, we now further investigate the junction dynamics directly via the characterization of device behavior in the phase diffusion regime. Phase diffusion manifests itself as an observable nonzero resistance below the critical current (even at $I_{\text{Bias}} = 0$), arising from phase slips that are caused by thermal noise. The rate of these phase slips down the prototypical titled washboard potential, and, therefore, the measured zero-bias resistance is governed by the junction dynamics which dictate the energy dissipation rate [18]. Indeed, we are able to observe a resistance in our devices, at zero bias, and down to 3 K in temperature. We define the measured zero-bias differential resistance as R_0. In order to confirm that R_0 arises from the phase diffusion mechanism, we study the evolution of this resistance with respect to temperature. Regardless of the junction damping dynamics the trend behavior of R_0 with respect to temperature should have the following dependence [5,18,21–25,27]:

$$R_0(T) \propto \frac{2E_J}{k_B T} e^{-2E_J/k_B T}. \tag{1}$$

Here, $E_J = \hbar I_C/2e$ is the Josephson energy. (The above exponential dependence holds when $2E_J/k_BT > 1$ [18].) Reworking Eq. (1), we can arrive at the proportionality relationship: $\ln(R_0T) \propto -2E_J/k_BT$. In Fig. 2(a) we plot the value R_0T versus inverse temperature T on a semilogarithmic scale. Indeed, we find that the relationship is nearly linear, consistent with theory. From here, knowing the temperature, we can extract E_J from the slope of the curves. The fitted Josephson energy versus gate voltage is plotted in Fig. 2(b). For single layer graphene Josephson junctions governed by ballistic transport it is expected that the value of E_JR_N is constant with respect to V_G [9]; and we find not only that indeed this is the case (see Fig. 2 inset), but also that this value matched well with the expected energy scale extracted

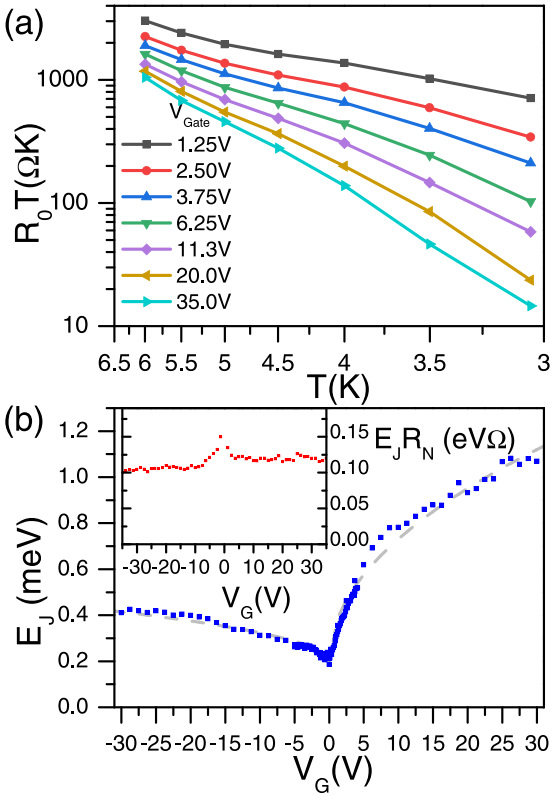

FIG. 2. (a) The product of temperature and the zero-bias resistance R_0T as a function of inverse temperature $1/T$ shown for several different gate voltages plotted on a semilogarithmic scale. The linear dependence of the curves shown here confirms that the resistance R_0 arises from the phase diffusion mechanism. (b) The Josephson energy E_J versus gate voltage V_G. Here E_J is calculated from the slope of the curves shown in panel (a). The dashed lines represent a square-root relationship between E_J and V_G (with an offset), the expected relationship for single layer graphene Josephson junctions in the long ballistic regime. (The inset) The product of the Josephson energy and normal resistance E_JR_N. For ballistic single layer graphene Josephson junctions, this product is expected to be constant with respect to gate voltage V_G.

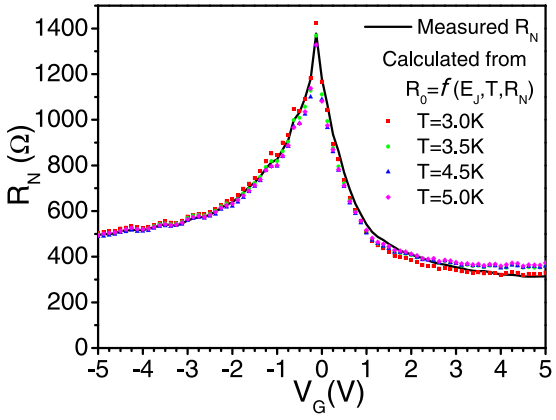

FIG. 3. Gate voltage dependence of measured normal resistance R_N (black line) compared to the resistance calculated from the theoretically predicted relationship between R_N and R_0: $R_N = R_0/[I_0(E_J/k_BT)]^{-2}$. ($I_0$ is the modified Bessel function.) R_N is measured at $I_{\text{Bias}} \gg I_S$ and is averaged for several data points for negative and positive biases. Here we present R_N measured at 3.5 K, however, at these temperatures the resistance shows negligible temperature dependence. The data and calculated result match well, supporting the claim that the measured device is an overdamped junction.

from the trend of I_S versus T (see Appendix C). Here R_N is the normal resistance, i.e., the resistance of the junction when it is in normal state. (The measured R_N can be found in Fig. 3.)

Having found the Josephson energy, we can determine the last parameter governing R_0. This final parameter is different depending on the damping dynamics of the junction. Previous theoretical works have defined three different regimes: For overdamped junctions, the governing parameter is R_N, the normal resistance [25,27]. For underdamped junctions, R_0 depends on the plasma frequency $\omega_p \propto \sqrt{E_J/C}$ [23]. (Here C is the capacitance of the junction.) Finally, if the junction is underdamped at low frequencies, but becomes overdamped at the plasma frequency (due to being shorted by the environment), we have $R_0 \propto Z_0$ [21]. Here Z_0 is the real part of the high-frequency impedance caused by the junction's environment [21]. We find that analyzing our devices as if they were underdamped or damped by the environment does not produce a good match between measured data and theoretical expectation. (See Appendix D).

Now, we confirm that our devices are indeed in the overdamped regime by comparing the measured normal resistance R_N with that backcalculated from the the zero-bias resistance R_0. Following the full expression in Ref. [27] we have

$$\lim_{I_{\text{Bias}}\to 0} \frac{V/I_{\text{Bias}}}{R_N} = \left[I_0\left(\frac{1}{2}\gamma\right)\right]^{-2}. \tag{2}$$

Here, I_0 is the modified Bessel function, and $\gamma = I_c\hbar/ek_BT$. (V is the voltage measured across the junction.) For I_{Bias} approaching zero, the equation simplifies to $R_N = R_0/[I_0(E_J/k_BT)]^{-2}$. Figure 3 shows the measured normal resistance R_N versus gate voltage V_G plotted together with the resistance calculated from Eq. (2) for different temperatures. It can be seen that we have a good match between the measured and the theoretical results, in particular, for high values of R_N.

The damping of the junction is typically determined by the quality factor Q with $Q = R_N(2eI_CC/\hbar)^{1/2} = \frac{2e}{\hbar}R_N\sqrt{E_JC}$. ($C$ being the capacitance of the junction.) A $Q < 0.85$ results in an overdamped junction [30]. If we assume that the net junction capacitance includes the contribution of the 100×100-μm bonding pads that couple to each other via the backgate below the 300-nm thick SiO_2 layer, we arrive at $C \approx 600$ fF. Taking the above capacitance, and the lowest measured values of $E_J = 0.3$ meV and $R_N = 100\ \Omega$, we arrive at a minimum quality factor of $Q = 1.6$: the underdamped regime. This estimate is contradictory to the observations above. In order for the junction to be overdamped, it needs to be adequately isolated from the bonding pads. At first glance, one may suspect that the resistance from the gold leads would be capable of sufficiently isolating the junction [13,31]. However, measurements of our leads show only 10 s of Ohms of resistance from the gold. Numerically solving the resistively capasitively shunted junction equations, whereas

including the effects of the bonding pads and leads show this is not enough to isolate the junction. In fact, the lead resistance would need to be near 500 Ω to sufficiently suppress hysteretic effects in the junction [11,32]. Instead, we believe that the junction is isolated through a series inductance, which, at the plasma frequency of our device (∼35 GHz) would need to be ∼2.2 nH. This inductance can be explained by the kinetic inductance of the disordered MoRe leads. Indeed, the room-temperature resistance of the MoRe is in excess of 10 $k\Omega$ indicating a high level of oxidation. The oxidation would introduce disorder, decreasing the Cooper pair density and, in turn, increasing the kinetic inductance. In fact, we estimate that given the lead room-temperature resistance, and the elevated temperature as compared to the superconducting gap, our leads have an inductance in excess of 10 nH (see Appendix B).

In conclusion, we have investigated the phase diffusion regime in hBN encapsulated graphene Josephson junction governed by ballistic electron transport. The observed trend of the measured zero-bias resistance R_0 with respect to carrier concentration conforms well to theory describing phase diffusion in an overdamped junction regime. This is a conclusive confirmation of overdamped behavior in graphene-based Josephson junction. We attribute this behavior to effective isolation of the Josephson junction from the capacitive contribution of the bonding pads. The isolation arises from an inductive connection within the device layout. In working towards applications of graphene-based superconducting devices in the field of quantum information [12–17] (e.g., quantum entanglers or parafermion-based qubits), a full description of the device behavior is required. This includes the design of the ture Josephson energy as well as controlling interaction with the environment. Our paper is an important step towards such environmental control.

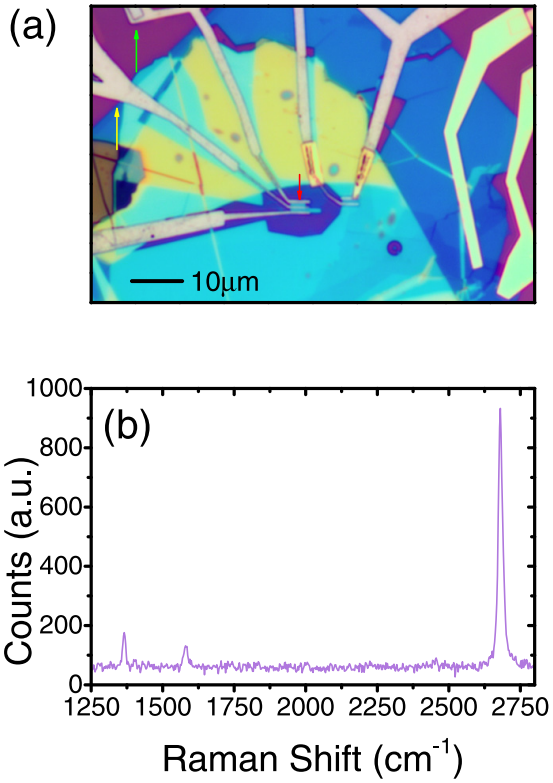

FIG. 4. (a) Optical image of the device presented in the main text. (Scale bar presented for reference). Graphene encapsulated in hBN acts as the normal metal portion of the device. The superconductor is made from MoRe alloy (yellow arrow) with the superconducting leads defining a junction of 500-nm length. The MoRe leads terminate ∼50 μm past the active area of the device. The bonding pads and leads connecting to the MoRe region are made of Cr/Au, thickness 5nm/110 nm). An example of the transition between MoRe and Cr/Au is highlighted by the green arrow. The red arrow indicated the junction presented in the main text. (b) The Raman spectrum of the graphene region used in the device.

ACKNOWLEDGMENTS

I.V.B. acknowledges funding from the Texas A&M University. J.T., A.Sh., and I.V.B. acknowledge CityU New Research Initiatives/Infrastructure Support from Central (APRC): 9610395, and the Hong Kong Research Grants Council Projects: (ECS) Projects No. 2301818 and (GRF) No. 11303619. Lithographic fabrication and characterization of the samples performed by E.G.A. and A.S. and were supported by the Division of Materials Sciences and Engineering, Office of Basic Energy Sciences, U.S. Department of Energy, under Award No. DE-SC0002765.

APPENDIX A: DEVICE DESIGN AND CHARACTERIZATION

The optical image of the device presented in the main text is shown in Fig. 4(a). Graphene is made using the exfoliation method [28], prior to encapsulation in (hBN the graphene is verified to be single layer using Raman spectroscopy [33]. The measured Raman spectrum is shown in Fig. 4(b). An AFM image is taken of the completed hBN-graphene-hBN stack (not shown), and an area free of bubbles and defects is chosen for further processing. Using CHF_3/O_2 plasma, the hBN-graphene-hBN stack is etched thorough in order to make quasi-one-dimensional electrical contacts with superconducting electrodes [14]. MoRe alloy electrodes are deposited onto the device using DC sputtering with the approximate thickness of 100–120 nm. [Yellow arrow in Fig. 4(a)]. The MoRe contacts define the Josephson junction dimensions. However, the MoRe leads are terminated ∼50 μm past the active area of the device. [Green arrow in Fig. 4(a)]. The bonding pads and thin metal leads making contact to MoRe are made of Cr/Au (5/110 nm).

APPENDIX B: ESTIMATION OF THE ISOLATING INDUCTANCE

As described in the main text in order for the junction to be in the overdamped regime, the junction must be isolated from the capacitance generated by the bonding pads and leads. In our device, we attribute the isolation to a large series kinetic inductance of the disordered MoRe film. Previous work [34], has shown that alloyed thin films can have substantial kinetic

inductance L_k. L_k can be estimated using Ref. [34],

$$L_K = \frac{l}{w}\frac{R_{sq}h}{2\pi^2\Delta}\frac{1}{\tanh\left(\frac{\Delta}{2k_BT}\right)}, \tag{B1}$$

where l and w are the length and width of the film, R_{sq} is the normal-state resistance, Δ is the gap, and T is the temperature. We measure the normal-state resistance of the film at room temperature to be $R_{sq} \gg 10$ kΩ, an indication the film is highly disordered. Based on the optical imaging in Fig. 4, the most likely region to host the disordered film is the dark gray region denoted by the yellow arrow. Therefore, the length and width are roughly 10 and 1 μm, respectively. The gap of MoRe is ∼1.3 meV. At 3 K, we estimate that this inductance is on the order of 10 nH; which at the plasma frequency of 35 GHz would result in an impedance of over 2 kΩ: substantially more than required to successfully isolate the junction from the bonding pads and leads.

APPENDIX C: SWITCHING CURRENT I_S DEPENDENCE ON TEMPERATURE T

In Josephson junctions, the measured switching current I_S is suppressed from the expected maximum critical current I_C with I_S found to be decreasing with increasing temperature T [18]. Measuring the trend of I_S with respect to temperature T, one can determine whether the junction is in the diffusive [6,35,36] or ballistic transport regime [9,37–43]. Additionally, by sweeping gate voltage V_G, one can also determine whether the junction is made of single layer or multilayer graphene. For the case of a Josephson junction governed by ballistic electron transport and with junction length $L \gtrapprox \xi$ (the superconducting coherence length) we expect that $I_S(T) \propto \exp(-k_BT/\delta E)$ [9,37–40]. The value of $\delta E \approx \hbar v_F/2\pi L$ is related to the Andreev bound states energy-level spacing ($E_0 = \pi\hbar v_F/L$) [18,37,38,44,45]. Here v_F is the the Fermi velocity; and in single layer graphene v_F is a constant with respect to carrier density. Therefore, δE is expected to be independent of the applied gate voltage V_G (as long as the junction remains ballistic). The trend of the switching current I_S versus temperature T can be seen in Fig. 5(a), plotted on a semilogarithmic scale for several values of V_G. A nearly linear decay can be observed. Fitting the data to the above exponential dependence, we can extract the value of δE. The guidelines of the fit result are shown as dashed lines in Fig. 5(a), whereas the fitted value of δE is presented in Fig. 5(b). One can see that δE is independent with respect to gate voltage V_G (aside from the expected deviations close to the Dirac point). Moreover, the extracted value is consistent with the designed length L of the junction [9]. As the temperature approaches zero, the switching current approaches the critical current with $I_CR_N = C\,\delta E$. (Here R_N is the normal resistance.) It has been found empirically, that the dimensionless proportionality constant C is ≈ 1 to 2, and is suppressed by the coefficient of transmission τ across the junction [9]. In Fig. 5(b), alongside δE, we plot the value of I_CR_N. The critical current I_C is backcalculated from the fitted Josephson energy E_J in the main text. Indeed, we find a good match between the two values. This suggests that our device is single layer graphene and is governed by ballistic electron transport. Moreover, that

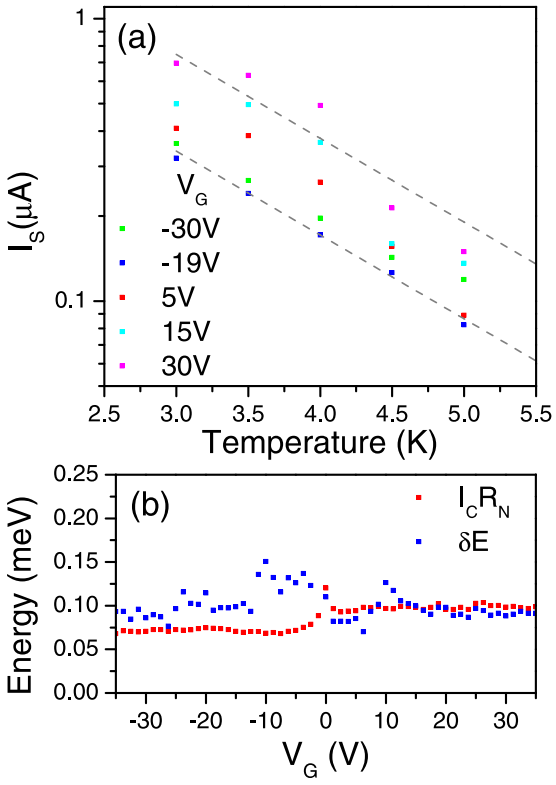

FIG. 5. (a) Switching current I_S versus temperature T plotted on a semilogarithmic scale. Plots for several values of gate voltage are shown. The plot shows a nearly linear decay with respect to T, from the slope of the decay one can fit the relevant energy scale δE. The fit results are plotted in panel (b), and as dashed guide lines in panel (a). (b)The fitted energy scale δE with respect to gate voltage V_G. A δE that is independent of gate is expected for single layer graphene. Alongside, is plotted the value I_CR_N (critical current times normal resistance). The two sets of data are very similar as is expected.

our fitted Josephson energy is close to the actual E_J of the device.

Had the device been in the diffusive regime, I_S would be governed by the Thouless energy, which has a more complicated relationship with respect to gate voltage. (A detailed investigation into the switching current and the governing parameters in garphene Josephson junctions can be found in Ref. [9] for ballistic devices and Ref. [6] for diffusive devices). The device shown in the main text largely follows the design parameters of those presented in Ref. [9].

APPENDIX D: COMPARISON TO UNDERDAMPED AND DAMPED BY ENVIRONMENT REGIMES

The main text presents the analysis of phase diffusion in the overdamped regime. Here we follow the analyses as if the Josephson junction was underdamped or damped by the environment at the plasma frequency. In following previous works, define the prefactor to the exponential in the main text Eq. (1) as a variable R_0' with $R_0' \equiv R_0 e^{(2E_J/k_BT)}$ [5]. For underdamped junctions, $R_0' \sim (h/e^2)\hbar\omega_p/k_BT$ [23], where $\omega_p \propto \sqrt{E_J/C}$ is the plasma frequency. Note that C is the capacitance of the junction and is a constant.) However, if the junction is

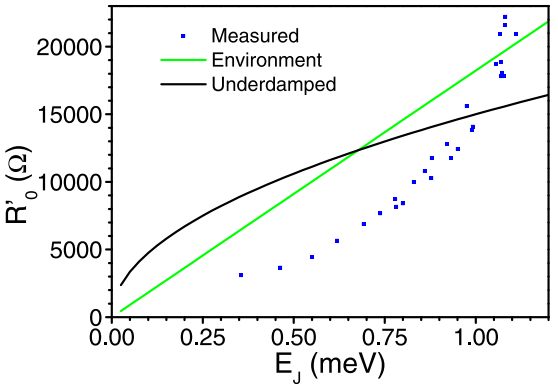

FIG. 6. The variable R_0' versus the Josephson energy E_J. The blue scatter data represent results obtained from the measured data. The black and green lines represent best-fit lines for the theoretical expectation in the case the Josephson junction is underdamped or damped by the environment (respectively). The mismatch between the measured data and theoretical predictions suggest than neither of these cases apply.

underdamped at low frequencies but becomes overdamped at the plasma frequency (due to being shorted by the environment), we have $R_0' = 2\pi Z_0 E_J/k_B T$ [21]. Here Z_0 is the real part of the high-frequency impedance caused by the junction's environment [21]. Typically Z_0 is found to be ∼200–250 Ω and can also be treated as a constant. (Note, that the above relationship holds only for $E_J > k_b T$ [21]). The measured R_0' versus the Josephson energy E_J is shown in Fig. 6 (data taken at 4.0 K). Alongside, we plot the best-fitting results obtained for each of the two cases mentioned above. Note that the trend of the measured result is superlinear; whereas the expected trend for the underdamped case is a square-root dependence, and a linear trend is expected in the damped by the environmental case. Clearly, the above two analyses do not apply. It is important to note that Ref. [5], erroneously used the same analysis via the variable R_0' for the overdamped case. This is not correct as the exponential dependence only approximates the slope of the trend with respect to temperature not the absolute value [18,27]. Instead, the full expression from Ref. [27] is to be used; as was performed in the ain text.

[1] H. B. Heersche, P. Jarillo-Herrero, J. B. Oostinga, L. M. K. Vandersypen, and A. F. Morpurgo, Bipolar supercurrent in graphene, Nature (London) **446**, 56 (2007).

[2] F. Miao, S. Wijeratne, Y. Zhang, U. C. Coskun, W. Bao, and C. N. Lau, Phase-coherent transport in graphene quantum billiards, Science **317**, 1530 (2007).

[3] X. Du, I. Skachko, and E. Y. Andrei, Josephson current and multiple andreev reflections in graphene sns junctions, Phys. Rev. B **77**, 184507 (2008).

[4] C. Ojeda-Aristizabal, M. Ferrier, S. Guéron, and H. Bouchiat, Tuning the proximity effect in a superconductor-graphene-superconductor junction, Phys. Rev. B **79**, 165436 (2009).

[5] I. V. Borzenets, U. C. Coskun, S. J. Jones, and G. Finkelstein, Phase Diffusion in Graphene-Based Josephson Junctions, Phys. Rev. Lett. **107**, 137005 (2011).

[6] C. T. Ke, I. V. Borzenets, A. W. Draelos, F. Amet, Y. Bomze, G. Jones, M. Craciun, S. Russo, M. Yamamoto, S. Tarucha, and G. Finkelstein, Critical current scaling in long diffusive graphene-based josephson junctions, Nano Lett. **16**, 4788 (2016).

[7] G.-H. Lee, D. Jeong, J.-H. Choi, Y.-J. Doh, and H.-J. Lee, Electrically Tunable Macroscopic Quantum Tunneling in a Graphene-Based Josephson Junction, Phys. Rev. Lett. **107**, 146605 (2011).

[8] U. C. Coskun, M. Brenner, T. Hymel, V. Vakaryuk, A. Levchenko, and A. Bezryadin, Distribution of Supercurrent Switching in Graphene under the Proximity Effect, Phys. Rev. Lett. **108**, 097003 (2012).

[9] I. V. Borzenets, F. Amet, C. T. Ke, A. W. Draelos, M. T. Wei, A. Seredinski, K. Watanabe, T. Taniguchi, Y. Bomze, M. Yamamoto, S. Tarucha, and G. Finkelstein, Ballistic Graphene Josephson Junctions from the Short to the Long Junction Regimes, Phys. Rev. Lett. **117**, 237002 (2016).

[10] M. B. Shalom, M. J. Zhu, V. I. Fal'ko, A. Mishchenko, A. V. Kretinin, K. S. Novoselov, C. R. Woods, K. Watanabe, T. Taniguchi, A. K. Geim, and J. R. Prance, Quantum oscillations of the critical current and high-field superconducting proximity in ballisticgraphene, Nat. Phys. **12**, 318 (2016).

[11] T. F. Q. Larson, L. Zhao, E. G. Arnault, M.-T. Wei, A. Seredinski, H. Li, K. Watanabe, T. Taniguchi, F. Amet, and G. Finkelstein, Zero crossing steps and anomalous shapiro maps in graphene josephson junctions, Nano Lett. **20**, 6998 (2020).

[12] I. V. Borzenets, Y. Shimazaki, G. F. Jones, M. F. Craciun, S. Russo, M. Yamamoto, and S. Tarucha, High efficiency CVD graphene-lead (pb) cooper pair splitter, Sci. Rep. **6**, 23051 (2016).

[13] I. V. Borzenets, U. C. Coskun, H. T. Mebrahtu, Y. V. Bomze, A. I. Smirnov, and G. Finkelstein, Phonon Bottleneck in Graphene-Based Josephson Junctions at Millikelvin Temperatures, Phys. Rev. Lett. **111**, 027001 (2013).

[14] F. Amet, C. T. Ke, I. V. Borzenets, J. Wang, K. Watanabe, T. Taniguchi, R. S. Deacon, M. Yamamoto, Y. Bomze, S. Tarucha, and G. Finkelstein, Supercurrent in the quantum hall regime, Science **352**, 966 (2016).

[15] M. T. Wei, A. W. Draelos, A. Seredinski, C. T. Ke, H. Li, Y. Mehta, K. Watanabe, T. Taniguchi, M. Yamamoto, S. Tarucha, G. Finkelstein, F. Amet, and I. V. Borzenets, Chiral quasiparticle tunneling between quantum hall edges in proximity with a superconductor, Phys. Rev. B **100**, 121403(R) (2019).

[16] G.-H. Lee, K.-F. Huang, D. K. Efetov, D. S. Wei, S. Hart, T. Taniguchi, K. Watanabe, A. Yacoby, and P. Kim, Inducing superconducting correlation in quantum hall edge states, Nat. Phys. **13**, 693 (2017).

[17] G.-H. Park, M. Kim, K. Watanabe, T. Taniguchi, and H.-J. Lee, Propagation of superconducting coherence via chiral quantum-hall edge channels, Sci. Rep. **7**, 10953 (2017).

[18] M. Tinkham, *Introduction to Superconductivity*, Dover Books on Physics Series (Dover, New York, 2004)

[19] T. A. Fulton and L. N. Dunkleberger, Lifetime of the zero-voltage state in josephson tunnel junctions, Phys. Rev. B **9**, 4760 (1974).

[20] J. Clarke, A. N. Cleland, M. H. Devoret, D. Esteve, and J. M. Martinis, Quantum mechanics of a macroscopic variable: The phase difference of a josephson junction, Science **239**, 992 (1988).

[21] G.-L. Ingold, H. Grabert, and U. Eberhardt, Cooper-pair current through ultrasmall josephson junctions, Phys. Rev. B **50**, 395 (1994).

[22] J. M. Martinis and R. L. Kautz, Classical Phase Diffusion in Small Hysteretic Josephson Junctions, Phys. Rev. Lett. **63**, 1507 (1989).

[23] R. L. Kautz and J. M. Martinis, Noise-affected i-v curves in small hysteretic josephson junctions, Phys. Rev. B **42**, 9903 (1990).

[24] Y. M. Ivanchenko and L. A. Zil'berman, JETP Lett **8**, 113 (1968).

[25] Y. M. Ivanchenko and L. A. Zil'berman, Sov. Phys. JETP **28**, 1272 (1969).

[26] L. Wang, I. Meric, P. Y. Huang, Q. Gao, Y. Gao, H. Tran, T. Taniguchi, K. Watanabe, L. M. Campos, D. A. Muller, J. Guo, P. Kim, J. Hone, K. L. Shepard, and C. R. Dean, One-dimensional electrical contact to a two-dimensional material, Science **342**, 614 (2013).

[27] V. Ambegaokar and B. I. Halperin, Voltage Due to Thermal Noise in the dc Josephson Effect, Phys. Rev. Lett. **22**, 1364 (1969).

[28] K. S. Novoselov, D. Jiang, F. Schedin, T. J. Booth, V. V. Khotkevich, S. V. Morozov, and A. K. Geim, Two-dimensional atomic crystals, Proc. Natl. Acad. Sci. USA **102**, 10451 (2005).

[29] H. Courtois, M. Meschke, J. T. Peltonen, and J. P. Pekola, Origin of Hysteresis in a Proximity Josephson Junction, Phys. Rev. Lett. **101**, 067002 (2008).

[30] K. K. Likharev, *Dynamics of Josephson Junctions and Circuits* (Gordon and Breach, Philadelphia, 1991).

[31] D. Vion, M. Götz, P. Joyez, D. Esteve, and M. H. Devoret, Thermal Activation above a Dissipation Barrier: Switching of a Small Josephson Junction, Phys. Rev. Lett. **77**, 3435 (1996).

[32] E. G. Arnault, T. F. Q. Larson, A. Seredinski, L. Zhao, S. Idris, A. McConnell, K. Watanabe, T. Taniguchi, I. V. Borzenets, F. Amet, and G. Finkelstein, Multiterminal inverse ac josephson effect, Nano Lett. **21**, 9668 (2021).

[33] A. C. Ferrari, J. C. Meyer, V. Scardaci, C. Casiraghi, M. Lazzeri, F. Mauri, S. Piscanec, D. Jiang, K. S. Novoselov, S. Roth, and A. K. Geim, Raman Spectrum of Graphene and Graphene Layers, Phys. Rev. Lett. **97**, 187401 (2006).

[34] A. J. Annunziata, D. F. Santavicca, L. Frunzio, G. Catelani, M. J. Rooks, A. Frydman, and D. E. Prober, Tunable superconducting nanoinductors, Nanotechnology **21**, 445202 (2010).

[35] P. Dubos, H. Courtois, B. Pannetier, F. K. Wilhelm, A. D. Zaikin, and G. Schön, Josephson critical current in a long mesoscopic s-n-s junction, Phys. Rev. B **63**, 064502 (2001).

[36] P. Dubos, H. Courtois, O. Buisson, and B. Pannetier, Coherent Low-Energy Charge Transport in a Diffusive S-N-S Junction, Phys. Rev. Lett. **87**, 206801 (2001).

[37] I. Kulik, Macroscopic quantization and the proximity effect in sns junctions, JETP **30**, 944 (1969).

[38] J. Bardeen and J. L. Johnson, Josephson current flow in pure superconducting-normal-superconducting junctions, Phys. Rev. B **5**, 72 (1972).

[39] A. Svidzinski, T. Antsygina, and E. Bratus, Superconducting current in wide sns junctions, JETP **34**, 860 (1972).

[40] A. V. Svidzinsky, T. N. Antsygina, and E. N. Bratus, Concerning the theory of the josephson effect in pureSNS junctions, J. Low Temp. Phys. **10**, 131 (1973).

[41] C. W. J. Beenakker, *Three "Universal" Mesoscopic Josephson Effects*, *Springer Series in Solid-State Sciences* (Springer, Berlin, Heidelberg, 1992), pp. 235–253.

[42] C. W. J. Beenakker and H. van Houten, Josephson Current Through a Superconducting Quantum Point Contact Shorter than the Coherence Length, Phys. Rev. Lett. **66**, 3056 (1991).

[43] G.-H. Lee, S. Kim, S.-H. Jhi, and H.-J. Lee, Ultimately short ballistic vertical graphene josephson junctions, Nat. Commun. **6**, 6181 (2015).

[44] A. Svidzinskii, *Spatially Inhomogeneous Problems in the Theory of Superconductivity* (Nauka, Moscow, 1982).

[45] A. A. Golubov, M. Y. Kupriyanov, and E. Il'ichev, The current-phase relation in josephson junctions, Rev. Mod. Phys. **76**, 411 (2004).